Ion beam sputter deposition technique for direct growth of Ge quantum dots on a graphene/SiO_2/Si substrate

Yu Yang*,**, Tianjian Zeng*, Zhang Zhang**, Chong Wang**, Tao Sun*

*School of Energy, Yunnan University, P. R. China, yuyang@ynu.edu.cn
** Institute of Optoelectronic Information Material, Yunnan University, P. R. China, taosun8805@163.com

ABSTRACT

The ion bean sputting deposition techinuqe has been successfully conducted directly for Ge quantum dots (QDs) grown on SiO_2/Si substrate. The results show that the morphology and size of Ge QDs on graphene can be modulated by tuning the Ge coverage. Compared with that of traditional Ge dots grownon Si substrate, the positions of both corresponding photoluminescence (PL) peaks of Ge QDs/graphene hybrid structure undergo a large red-shift, which can probably be attributed to the lack of atomic intermixing and the existence of surface states in this hybrid material. According to DFT calculations, the Ge growth on the graphene follows the so-called Volmer–Weber mode. The therotical studies results illustrated that the interaction between Ge and graphene layer can be enhanced with the decrease of the Ge coverage. This project may supply a prototype for QDs/graphene hybrid nanostructure material fabricating for optoelectronic devices.

Keywords: ion beam sputtering deposition, charges transfer, Ge QDs/graphene, first-principles calculations

1 INTRODUCTION

The quantum dots (QDs)/graphene hybrid structure shows excellent photoresponse properties in the photodefectivity devices, which caused by effects of the unique QDs quantum confinement and the ultrahigh carrier mobility of graphene.[1-3] Thus, this project invented the ion beam sputtering deposition technique (IBSD) to realize the directly growth of Ge quantum dots (QDs) on single-layer graphene on a SiO_2/Si as the substrate.[4-6]

The morphology results illustrate that the Ge QDs size and morphology on graphene can be modulated via tuning the Ge coverage by IBSD technique. The results also indicate that increasing the sputtering time of Ge, the density of Ge dots increased, but the sizes of Ge dots tend to decrease.[7] All morphology evolution route of Ge islands agrees well with the Zinsmeister theory.[6, 8-10] Secondly, the existence of interaction like doping effects at the interface of Ge QDs with graphene has been demonstrated. The strength of the interaction can be enhanced remarkably by reducing the Ge coverage in a certain scope, which indicates that the interaction can be modulated via controlling the coverage of Ge. The charge transfer behaviour at the interface of Ge/graphene also has been demonstrated. Comparing with traditional methods for Ge dots grown on Si substrate, the IBSD treatment changes the positions of corresponding PL peaks of Ge QDs/ graphene hybrid structure undergo a large red-shift, which was attributed to the lack of atomic intermixing and the existence of surface states in this hybrid material. According to DFT study, the Ge growth on the graphene follows the Volmer–Weber mode instead of the traditional Ge QDs/Si system Stranski–Krastanow mode.[11, 12] The theoretical study also suggests that decreasing the Ge coverage enhances the interaction between Ge and graphene layer, which highly agree with the experimental results.

The final products were applied in a FET photodetectors, the device demonstrates the responsivity of 4.3 AW^{-1} at 808nm infrared light irradiation and relatively large values (0.92) of β in absolute. The optoelectronic features indicate that the device using IBSD fabricated Ge QDs/graphene improves the efficiency of carrier transfer and overcome the limit of ligand barrier at the interface of Ge/graphene. This project supplies a new technique for fabricating hybrid nanostructure QDs/graphene for novel optoelectronic devices application.

2 EXPERIMENTAL

The IBSD technique were applied for directly grown the Ge dots on graphene. Before the deposition, the SiO_2/Si substrates with the thickness of a 500 μm n-type silicon wafer and a 300 nm SiO_2 capping layer were carefully cleaned following the standard Shraki process. Then, the CVD-grown graphene was transferred onto the SiO_2 film surface. A Kaufman-type ion source, 30 nm in calibre, was used to produce the Ar ion beam. The background and deposited pressures were 2.3×10^{-6} and 1.5×10^{-6} Torri respectively. The current value and the ion energy were set to sputter the Ge targets at 7 mA and 1 keV. The average deposited rates of Ge were 0.07 ML. The growth experiments were carried out at room temperature and 500 °C. Three Ge QDs/graphene samples grown at RT and with the different deposition durations of 60, 180, and 300 s, are named as sample A_{RT}, B_{RT}, and C_{RT} respectively. The fourth sample grown at 500 °C and with duration of 180 s is named as B_{500}. The morphologies of all samples were characterized by AFM technique. Raman spectra were conducted with the excitation wavelength of 514.5 nm. PL signals of these samples were measured by using the 532 nm-line laser as excitation source. X-ray photoelectron

spectroscopy (XPS) experiments were carried out by a PHI-5400 XPS instrument using a monochromatized Al-Kα x-ray source. The energetic band XPS corresponding to the 3d core level of Ge was obtained at an angle of 45°; the vacuum chamber was chosen at 10^{-7} Pa during the measurements.

3 RESULTS AND DISCUSSION

Figure 1 illustrates that the Ge QDs size and morphology on graphene can be modulated via tuning the Ge coverage by IBSD technique, it indicates that the Ge atoms incorporate with each other on the graphene surface to form the nucleation at firstly, then evolve into Ge islands at the nucleation sites by gathering subsequent atoms. It also indicates that the Ge QD sizes and density can be modulated by the sputtering time of Ge.

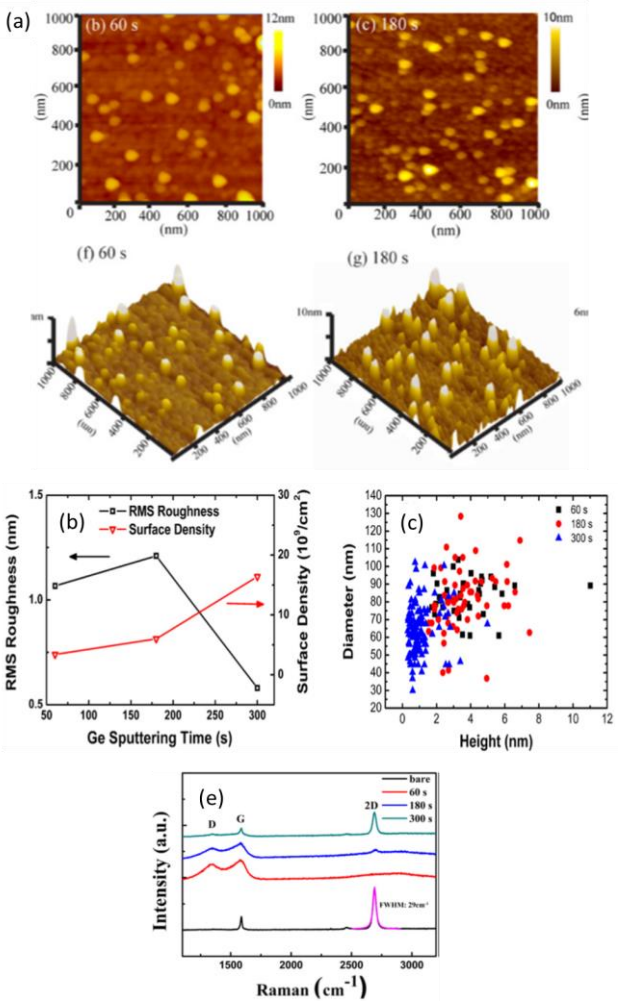

Figure 1: (a) AFM top-view images of surface morphologies with 60s and 80s deposition time of Ge on graphene, (b) Evolution of surface RMS roughness and density depending on sputtering time of Ge, (c) Scatter plot of diameter and height of dots for different Ge sputtering time samples grown at room temperature, (e) Comparison of Raman spectra at 514 nm for deposited Ge on graphene during different sputtering time. [12]

In the sample with the sputtering time of 300 s, it is interesting to note that the mean height of Ge QDs decreases to 1.8 nm, this may be related to the formation of massive islands with smaller sizes on the graphene. According to the observations above, it can be concluded that the morphologies of Ge QDs are modulated by the sputtering time of the Ge layer. With the increase of sputtering time from 60 to 300 s, the island density increase monotonously, while the surface roughness slightly increases at first, then decreases again. To some extent, this behaviour of roughness can probably be attributed to the rapid formation of small and compact islands grown on graphene.[12]

The Raman spectra of bare graphene, Sample A_{RT}, B_{RT}, and C_{RT} are all shown in figure 1 (e). For the bare graphene sample, the two most intense features, 2D peak and G peak, are observed at 2692 and 1589 cm^{-1} respectively. For the three samples ART, BRT, and CRT, a new peak labelled as 'D' appears at 1347 cm^{-1} in their Raman spectra. The D peak can be attributed to defects that are probably introduced in the sputtering process. The highly energetic Ge atoms make the carbon atoms in graphene deviate away from their equilibrium. This kind of collision leads to the formation of a certain number of defects. Compared with that of the bare graphene, the 2D and G peak of the three QDs/graphene samples undergo an obvious red-shift and blue-shift respectively.

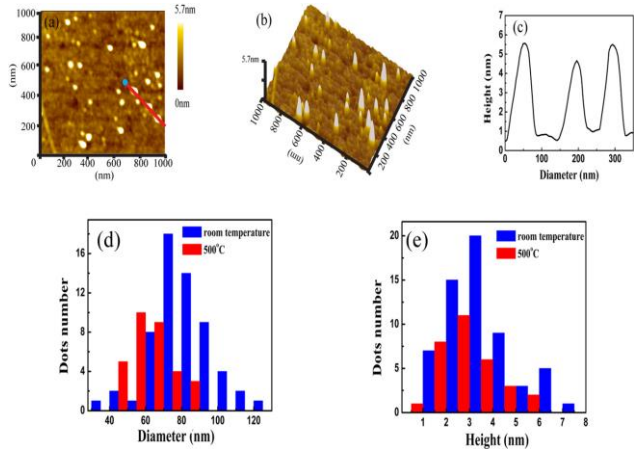

Figure 2: (a) AFM top image of Ge grown on graphene at 500 °C, the sputtering time is 180 s (scale bar was given beside). (b) The 3D AFM image of Ge QDs grown at 500 °C during the sputtering time of 180 s. (c) The height profile along the red line labelled in (a); the blue dot in (a) marks the zero point in (c). (d) Distribution of diameter of Ge QDs on graphene. (e) Height distribution of Ge QDs on graphene.

In order to improve the crystalline quality of Ge QDs, growing temperature is increased to 500°C. Figure 2(a-b) shows the AFM images of sample B_{500} with the sputtering time of 180s. Comparing with other samples grown at room temperature, the Ge QDs fabricated at 500°C is less density and has better size uniformity. Figure 2(a) shows the AFM images of sample B_{500} with the sputtering time of 180 s. Ge

QDs with less density and better size uniformity are observed, compared with those in samples grown at room temperature. The average diameter and height of Ge QDs in this sample are 59.5nm and 3.2 nm respectively. At the same time, the dots density is reduced to 3.6 × 109 cm^{-2} obtained from the counting in figure 2(a). Figure 2(b) shows the 3D AFM image of this sample. The 3D morphology of the Ge QDs gives the evidence for the direct growth of 3D Ge QDs on graphene. Figure 2(c) is height profile of three QDs' boundary dimension along the red scanning line labeled in figure 2(a). The size of the dots along the line exhibits good uniformity. Figures 2(d) and (e) show the distribution of diameter and height, respectively, of Ge QDs on graphene extracted from figure 2(a). Compared with that of the samples grown at room temperature, the statistical results indicate that the average sizes of QDs in Sample B_{500} decrease. Meanwhile, the dot density also reduces with increasing temperature to 500 °C.

The increasing growth temperature enhances the kinetic energy and the mobility of the Ge atoms and also increases the chance of desorption of Ge atoms from graphene surface and collision probability between Ge atoms. Subsequently the size and density of Ge islands shrink as in the observation in sample B_{500}. Similar phenomena have also occurred in our other QDs/graphene samples with growth temperature of 600°C and 700 °C in which the dot density and size are less than that in Sample B_{500}. The higher mobility of Ge atoms also accelerates the incorporation of small Ge QDs and leaves relatively large QDs on graphene.[12] This could be the major factor which is responsible for the uniformity of Ge QDs.

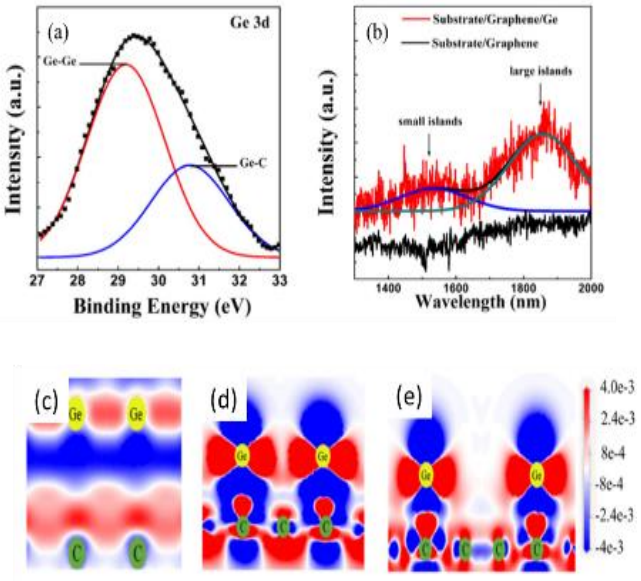

Figure 3: (a) Narrow scan of XPS Ge QDs grown on graphene surface; (b) PL spectra measured at the excitation of 532nm laser from the sample grown at 500°C on SiO_2/Si substrate with (without) Ge deposited on graphene; Charge density redistribution in Ge monolayer interacting with different coverage (c) θ = 1/2. (d) θ = 1/8. (e) θ = 1/18.

The existence of interaction such as doping effects at the interface of Ge QDs with graphene has been demonstrated also. The strength of the interaction can be enhanced remarkably by reducing the Ge coverage in a certain scope, which indicates that the interaction can be modulated via controlling the coverage of Ge (Figure 3(a)). Figure 3(b) illustrates that the charge transfer behaviour of doping effect in graphene. Comparing with traditional methods for Ge dots grown on Si substrate, the IBSD treatment changes the positions of corresponding photoluminescence (PL) peaks of Ge QDs/graphene hybrid structure undergo a large red-shift, which was attributed to the lack of atomic intermixing and the existence of surface states in this hybrid material.

To reveal the interaction between Ge adatoms and graphen further, the charge redistribution of the three coverage cases are also calculated, as shown in figure 6. The results show that when coverage θ = 1/2, charges accumulate between two Ge adatoms while depopulate at the interface of Ge/graphene, as seen in figure 3(c). It is inferred that the strong adatom–adatom interaction leads Ge atoms to adsorb weakly on graphene and the interaction strength between Ge and graphene is suppressed greatly.[12] With lowering the of coverage to θ = 1/8, the localization of charges between Ge and C atoms has been strengthened, as shown in figure 3(d), indicating Ge adatoms have a stronger interaction with graphene compared to high coverage cases. However, it is worthy of note that a weak interaction between two Ge adatoms is still present due to tiny charge accumulation remaining between Ge atoms. When coverage reduces θ = 1/18, the adsorption becomes dominant and the adatom–adatom interaction can be neglected here. The adsorption energy calculated in this condition is reliable. At the same time, the accumulation and depopulation of the charges at the interface are displayed clearly as shown in figure 3(e).

When the coverage is relatively high, the interaction of Ge–graphene will be suppressed by that of Ge–Ge. Therefore, the results calculated in such situations can not be used to predict the growth morphology of Ge on graphene based on the ratio of *Ea/Ec*. Reasonably, we choose to use the adsorption energy Ea of coverage θ = 1/18 from our calculation and bulk cohesive energy *Ec* (−3.85 eV) to obtain the ratio of Ea/Ec. Based on the analysis before, the system of Ge adatoms on graphene has a low ratio *Ea/Ec* = 0.19. This value is smaller than that of metals favoring 3D islands morphology reported. So it is reasonable to predict that the growth of Ge on graphene should tend to produce 3D islands. In addition, the localization of charge redistribution becomes the highest. According to the first principle calculation (Figure 3(c-e)), the Ge growth on the graphene follows the Volmer–Weber mode instead of the traditional Ge QDs/Si system Stranski–Krastanow mode.[5, 12] The theoretical study also suggests that decreasing the Ge coverage enhances the interaction between Ge and graphene layer, which highly agree with the experimental results.Fortunately, this theoretical

prediction agrees well with our experimental observations in AFM images.

The final produced materials were applied in a FET photodetectors, the device demonstrates the responsivity of 4.3 AW^{-1} at 808nm infrared light irradiation and relatively large values (0.92) of β in absolute. The optoelectronic features indicate that the device using IBSD fabricated Ge QDs/graphene improves the efficiency of carrier transfer and overcome the limit of ligand barrier at the interface of Ge/graphene.

4 CONCLUSION

The IBSD methods for directly growth Ge on graphene layer has been successfully. The results indicate that modification the sysnthesis conditions could imporve the quanlity and quantity of QDs on SiO_2/Si substrate, these path including increasing the sputtering time of Ge, changing the sizes of Ge dots. The morphology evolution of Ge islands well agreed with the Zinsmeister theory. The strength of the interaction can be remarkably enhanced by reducing the Ge coverage in a certain scope, this indicates that the interaction can be modulated by controlling the coverage of Ge. However, the defects are introduced to the graphene layer more while the interaction enhanced. Comparing with the sample grown at room temperature, the sizes of Ge dots decrease with the increase of growth temperature. , there was an extremely large red-shift of the two PL peaks from the Ge QDs has been demonstrated in the PL spectra of the Ge QDs/graphene system, which probably casued by the lack of atomic intermixing and the existence of surface states in the Ge QDs/graphene hybrid structure. According to the therotical study results, the semiconductor Ge tends to undergo a 3D growth on the graphene surface. The interaction strength between 3D Ge QDs and graphene layer can be enhanced by decreasing the Ge coverage. This project serves an important step to realize high performance optoelectronic devices based on QDs/graphene hybrid nanostructures.

ACKNOWLEDGEMENTS

This work were financially supported by National Science Foundation of China (No. 10990103 and 11274266), the Open Project launched by National Laboratory for Infrared Physics (No. M201405), and the Key Project of Applied Basic Research Project of Yunnan Province of China (No. 2013FA029), the Scientific Research Key Fund of Yunnan Provincial Department of Education (No. 2015Z002 and 2015Z017). The authors thank the high-performance computing enter of Yunnan University for providing computational resources.

REFERENCES

[1]. Turyanska, L., et al., *Ligand-Induced Control of Photoconductive Gain and Doping in a Hybrid Graphene-Quantum Dot Transistor.* Advanced Electronic Materials, 2015. **1**(7): p. 1500062.

[2]. Zhang, L., et al., *Aptamer-mediated nanocomposites of semiconductor quantum dots and graphene oxide as well as their applications in intracellular imaging and targeted drug delivery.* J. Mater. Chem. B, 2014. **2**(48): p. 8558-8565.

[3]. Zhao, K., et al., *SnO_2 Quantum Dots@Graphene Oxide as a High-Rate and Long-Life Anode Material for Lithium-Ion Batteries.* Small, 2016. **12**(5): p. 588-594.

[4]. Konstantatos, G., et al., *Hybrid graphene-quantum dot phototransistors with ultrahigh gain.* Nat Nanotechnol, 2012. **7**(6): p. 363-368.

[5]. Wang, C., et al., *Electronic properties of single Ge/Si quantum dot grown by ion beam sputtering deposition.* Nanotechnology, 2015. **26**(10): p. 105201.

[6]. Xiao, F.X., J. Miao, and B. Liu, *Layer-by-layer self-assembly of CdS quantum dots/graphene nanosheets hybrid films for photoelectrochemical and photocatalytic applications.* J Am Chem Soc, 2014. **136**(4): p. 1559-1569.

[7]. Wang, R., et al., *Structure and luminescent property of Er^{3+}-doped germanate glasses.* Journal of Non-crystalline Solids, 2014. **383**: p. 200-204.

[8]. Gao, Y., et al., *Hybrid Graphene-Giant Nanocrystal Quantum Dot Assemblies with Highly Efficient Biexciton Emission.* Advanced Optical Materials, 2015. **3**(1): p. 39-43.

[9]. Malak, S.T., et al., *Large-Area Multicolor Emissive Patterns of Quantum Dot-Polymer Films via Targeted Recovery of Emission Signature.* Advanced Optical Materials, 2016. **4**(4): p. 608-619.

[10]. Bonaccorso, F., et al., *Graphene photonics and optoelectronics.* Nature Photonics, 2010. **4**(9): p. 611-622.

[11]. Yu, T., et al., *Graphene Coupled with Silicon Quantum Dots for High-Performance Bulk-Silicon-Based Schottky-Junction Photodetectors.* Adv Mater, 2016. **28**(24): p. 4912-9.

[12]. Zhang, Z., et al., *Direct growth of Ge quantum dots on a graphene/SiO_2/Si structure using ion beam sputtering deposition.* Nanotechnology, 2016. **27**(30): p. 305601.